Journal of Building Engineering 104 (2025) 112328

Contents lists available at ScienceDirect

Journal of Building Engineering

journal homepage: www.elsevier.com/locate/jobe

Seismic vulnerability and fragility assessment of masonry structures within the historic centre of Meta (Naples, Southern Italy)

Luigi Amitrano, Roberta Di Chicco, Antonio Formisano [*]

Department of Structures for Engineering and Architecture, University of Naples "Federico II", Italy

A R T I C L E I N F O

Keywords:
Masonry structures
Seismic vulnerability
CARTIS survey form
Seismic risk analysis
Fragility curves
Damage scenario

A B S T R A C T

The study presents a comprehensive analysis of the structural typologies and seismic vulnerability of the built environment within the municipality of Meta (Naples, Campania region of Italy), focusing on masonry structures found in the historical centre. Due to the high percentage of ancient masonry buildings designed without seismic criteria, the study, adopting the CARTIS survey form-developed within the DPC–ReLUIS Italian research project-investigates the key structural features that can affect the buildings' seismic response, such as construction material and typological configuration. The vulnerability assessment is then performed following a vulnerability index-based approach that uses a survey form conceived for aggregated buildings. Expected damage scenarios, useful for seismic risk analysis, are simulated by selecting six seismic events from the INGV's (National Institute of Geophysics and Volcanology) seismic hazard map for Meta and using a seismic intensity prediction equation. Finally, fragility curves are derived with a macroseismic approach for three different identified CARTIS masonry typologies, named MUR1, MUR2, and MUR3, highlighting the different probabilities of exceeding the various damage states.

1. Introduction

The Italian territory is renowned for its significant seismic activity, which poses considerable challenges for historical areas, as evidenced by the seismic events of 2009 and 2016 [1,2]. Historic centres, typically composed of ancient masonry buildings, reflect construction practices predating modern seismic codes. Consequently, these structures were designed to withstand only vertical loads and generally exhibit poor resistance to horizontal forces, such as those induced by seismic ground motion. Factors such as geometric complexity, material heterogeneity, and the absence of seismic protection measures further reduce their seismic safety [1,3]. As a result, seismic risk in historic Italian areas is categorized as medium to high [4].

Masonry structures in historic centres exhibit various characteristics that influence their seismic performance. The material composition of masonry walls, construction techniques, and architectural configurations significantly affect structural behaviour. Heterogeneous materials, such as stone and brick combined with variable-quality mortar, result in inconsistent mechanical properties and stress distributions. Irregular layouts further complicate seismic resistance. Additionally, centuries of insufficient maintenance and a lack of seismic strengthening exacerbate their vulnerabilities [3,5].

* Corresponding author.
E-mail address: antoform@unina.it (A. Formisano).

https://doi.org/10.1016/j.jobe.2025.112328
Received 5 February 2025; Received in revised form 21 February 2025; Accepted 8 March 2025
Available online 12 March 2025

Urban sprawl has shaped historical centres over time, often resulting in densely packed building aggregates. These aggregates consist of adjacent buildings sharing common walls, which interact dynamically during seismic events, leading to complex failure modes. Dynamic interactions, such as hammering and differential movement, are challenging to model accurately. Aggregates are also characterized by variations in construction age, materials, heights, and storey configurations, further increasing vulnerability. Numerous studies have highlighted that these structures require more detailed analysis than isolated buildings, as seismic events often trigger cascading failures within aggregates [3,5,6].

Given these challenges, a systematic approach to assessing the seismic vulnerability of masonry buildings is essential. In Italy, the CARTIS survey form is a primary tool for this purpose. Developed within the DPC–ReLUIS research project, CARTIS provides a standardized yet adaptable framework for categorizing building types and assessing seismic vulnerabilities. It incorporates parameters such as structural typology, preservation state, and geometric characteristics, facilitating comparative analyses across different urban areas [7].

Current literature identifies empirical, numerical, and hybrid methodologies for seismic vulnerability assessment [8–10]. Empirical methods rely on statistical analyses of post-earthquake data to define vulnerability classes, grouping buildings by shared construction features and typical damage patterns. These methods use macroseismic intensity to estimate seismic response, incorporating factors such as aggregate position. Vulnerability index-based approaches are a prominent example, offering systematic procedures implemented in various studies [11].

This study focuses on assessing the seismic vulnerability of the building stock in Meta, a municipality in the Campania region of Italy. Meta serves as a representative case study due to its concentration of masonry structures and unique vulnerabilities. Using the CARTIS form, data such as vertical structural materials and floor configurations were collected, statistically processed, and integrated into QGIS [12]. The analysis concentrated on the historic centre, employing a vulnerability index-based approach to predict damage scenarios through intensity prediction equations. Key outcomes include typological fragility curves derived using macroseismic approaches and urban vulnerability maps, which are critical for seismic risk analysis and mitigation.

Data collection for Meta's historic centre utilized the 1998 municipal building registry [13], which provided foundational structural information. To enhance this dataset, external on-site inspections were conducted, though access limitations restricted more detailed assessments. QGIS played a central role in visualizing spatial data, enabling the creation of thematic maps illustrating vulnerability indices and potential damage distributions. These spatial analyses aid in assessing risk distribution and prioritizing interventions.

Based on the collected data and structural classifications, probabilistic fragility curves were developed for the masonry typologies (MUR1, MUR2, and MUR3) identified in Meta's historic centre. Fragility curves quantify the probability of a structure reaching specific damage states under varying seismic intensities, providing insights into the performance of different masonry types. These curves were calibrated using empirical data and regional seismic models, offering realistic vulnerability estimations tailored to Meta's local

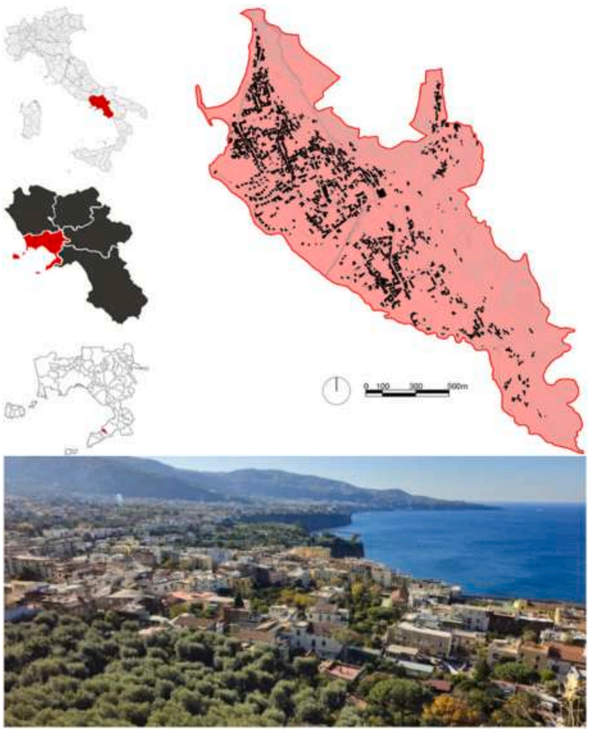

Fig. 1. Location and bird-eye view of the municipality of Meta.

context. Probabilistic methods also accounted for uncertainties in material properties, construction quality, and seismic hazard. The resulting fragility curves inform both engineering evaluations and policy-making, enabling targeted interventions to improve seismic resilience and preservation [8,9,14].

In conclusion, this study provides a comprehensive framework for understanding and mitigating seismic risk in historic masonry buildings. The integration of CARTIS assessments, GIS-based visualization, and probabilistic analyses offers a robust approach for characterizing vulnerabilities and supporting sustainable preservation strategies.

2. Analysis of the Meta's building stock: the CARTIS procedure

The municipality of Meta is one of six municipalities located on the Sorrento Peninsula. Despite its small territorial size of 2.25 km^2, Meta boasts a diverse geographical setting. It is bordered by the Lattari Mountains to the north, Monte Vico Alvano to the southeast, the

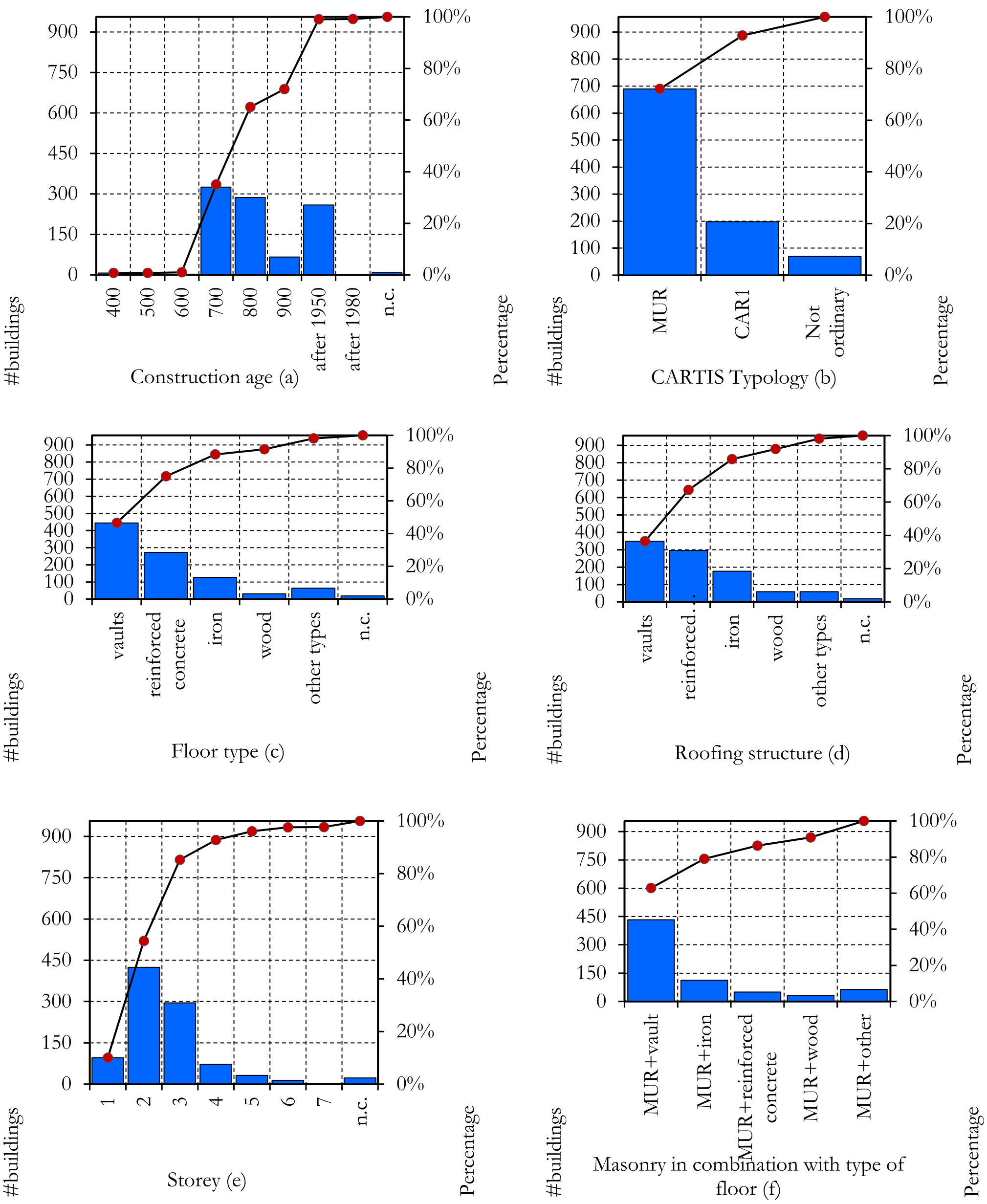

Fig. 2. Key structural features of Meta's building stock: (a) construction age, (b) CARTIS typology, (c) floor type, (d) roofing structure, (e) storey, (f) masonry in combination with type of floor.

Vallone dei Mulini di Meta to the south (which separates it from the municipality of Piano di Sorrento), and the sea to the northwest (see Fig. 1). According to the latest ISTAT data [15], Meta has a population of 7727 people, resulting in a high population density of approximately 3434 inhabitants per km^2.

To assess the seismic vulnerability of Meta's building stock, this study employed the first-level CARTIS form. The form is designed to identify areas with homogeneous building fabric by considering factors such as construction age and prevalent structural techniques. Developed under the ReLUIS 2014–2016 project, titled "Development of a Systematic Methodology for Exposure Assessment at a Territorial Scale Based on Typological/Structural Characteristics of Buildings," the CARTIS methodology was created in collaboration with the Department of Civil Protection (DPC). It integrates previous research by the Naples Research Unit (now part of the PLINIVS/LUPT Study Centre) and the National Seismic Service, now the DPC's Office for Seismic and Volcanic Risk.

The first-level CARTIS form consists of four sections: Section 0 (municipality and urban sector identification), Section 1 (building types), Section 2 (general building characteristics), and Section 3 (detailed typological characterization). Following this, the second-level CARTIS form was used to collect more detailed data on individual buildings. This form, also divided into four sections, includes information on the municipality and building location (Section 0), building identification (Section 1), general characteristics (Section 2), and structural element characterization (Section 3) [7,16,17].

The study is focused on ordinary buildings, primarily multi-story structures intended for residential or service-oriented use, with masonry or reinforced concrete frameworks, low inter-floor heights, and closely spaced walls. These structures, also covered by the AeDES manual (post-earthquake damage and safety assessment), are chosen for their comparability with other residential buildings. Monumental structures, industrial and commercial buildings, and strategic facilities, such as hospitals and government offices, are excluded due to their distinct structural characteristics [18].

Data collection is based on the 1998 Building Registry of Meta, referenced in the municipality's General Plan (PRG), which includes 956 buildings. The findings are as follows: most buildings in Meta date back to before the 20th century, with 34 % built in the 18th century, 30 % in the 19th century, and 27 % after 1950. In the registry, 72.1 % of buildings have masonry (MUR) vertical structures, 20.7 % are made of reinforced concrete (CAR1), and the remaining 7.2 % consist of materials such as wood, steel, or mixed materials [13]. As shown in Fig. 2f, only buildings with masonry structures, totalling 689, are considered for further analysis.

Preliminary findings suggest that buildings with vertical masonry structures and deformable or semi-deformable floors, including the vaults characteristic of historic masonry constructions, are expected to exhibit high seismic vulnerability. Research indicates that while vaults are effective in supporting vertical loads, they provide limited lateral resistance, making them particularly prone to seismic forces [19,20]. For example, seismic activity can cause cracking or even collapse in vaults due to their low tensile strength, as demonstrated by Puncello and Caprili (2023) and Ferretti et al. (2024) [19,20]. The size-effect also plays a fundamental role on the vulnerability of masonry vaults [21]. In contrast, masonry buildings with rigid reinforced concrete floors tend to perform better during seismic events. These floors enhance the building's box-like structural behavior, improving its resistance to lateral forces and significantly reducing the risk of collapse [19,20,22]. This highlights the crucial role of floor rigidity in mitigating the seismic vulnerability of masonry buildings.

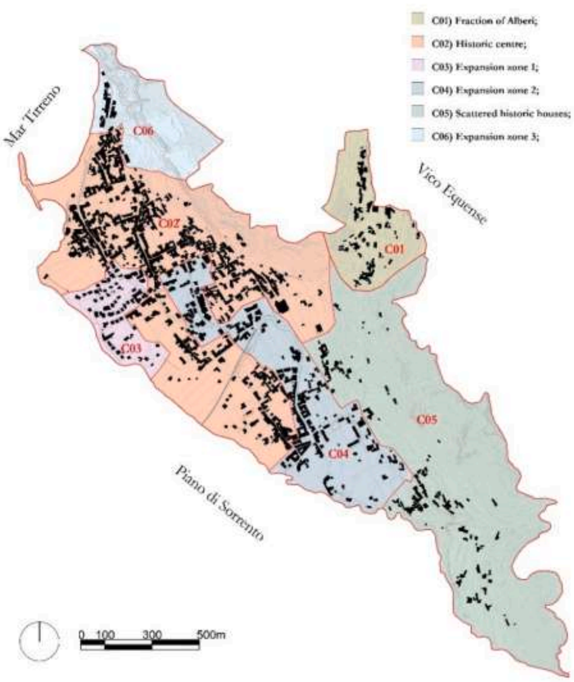

Fig. 3. Urban sectors identified in the territory of Meta.

2.1. Identification of the urban sectors

Following the CARTIS procedure [16], the municipality of Meta has been divided into six urban sectors, each characterized by distinct construction periods and structural typologies (see Fig. 3). These sectors were identified based on the predominant building features in each area, with a focus on construction age and the vertical structure of buildings. This compartmentalization provides a detailed understanding of the structural vulnerabilities within Meta, facilitating more targeted assessments and potential interventions.

The first sector, the Fraction of Alberi (C01), consists of 61 buildings. The majority of these buildings date back to the 1800s (42.6 %) or were constructed after 1950 (31.2 %), with a smaller proportion built in the 1900s (18.0 %). The dominant structural typology in this sector is masonry (MUR), accounting for 72.1 % of the buildings, while reinforced concrete (CAR) makes up 19.7 %, and the remaining 8.2 % are classified under other types. Vaults are the most common horizontal structure (45.9 %), followed by reinforced concrete slabs (31.1 %). This trend is also evident in the roof structures, where vaults constitute 41.0 %, reinforced concrete 34.4 %, and steel 16.4 %. The buildings are primarily two-story (57.4 %), with smaller proportions of three-story (23.0 %) and single-story (14.8 %) structures.

The second sector (C02), the historic centre of Meta, is the focus of a detailed analysis in the following sections of this paper. The third sector, Expansion Zone 1 (C03), consists of 64 buildings, most of which were constructed after 1950, accounting for 82.8 % of the structures. Only a small proportion was built in the 1900s (6.3 %). In this sector, masonry (MUR) typologies dominate, making up 73.4 % of the buildings, while reinforced concrete (CAR) accounts for 23.4 %. Reinforced concrete is predominantly used in both horizontal (81.3 %) and roof structures, with minor contributions from wood and steel (9.4 %). Building heights are generally two-story (45.3 %), with smaller proportions of three-story (29.7 %) and single-story (9.4 %) structures.

Expansion Zone 2 (C04) is the largest sector, encompassing 178 buildings with a balanced distribution of construction periods. Of these, 44.4 % were built after 1950, 24.7 % in the 1800s, and 23.0 % in the 1900s. Masonry (MUR) is the dominant structural type, representing 56.7 % of the buildings, while reinforced concrete (CAR) makes up 36.0 %. Reinforced concrete is predominant in both horizontal (44.4 %) and roof structures (45.5 %), although vaults (28.7 % in horizontal, 21.9 % in roof) and iron (18.0 %) also play significant roles. The buildings in this sector are mostly two-story (36.5 %), with significant proportions of three-story buildings (28.1 %) and a smaller number of taller structures (4–5 floors, around 10 %).

The fourth sector, Scattered Historic Houses (C05), consists of 113 buildings, with most constructions dating from the 1700s (47.8 %) and 1800s (26.6 %), while a smaller proportion were built after 1950 (16.8 %). This sector shows a strong prevalence of masonry (MUR) structures, which make up 86.7 % of the buildings. Vaults dominate both horizontal (48.7 %) and roof structures (41.6 %). Buildings are primarily two-story (47.8 %) or three-story (23.1 %), with a similar proportion of single-story buildings (23.1 %).

The final sector, Expansion Zone 3 (C06), is the smallest, with only 25 buildings. The majority of these structures were built after 1950 (76.0 %), with a smaller proportion from the 1800s (12.0 %) and 1700s (8.0 %). The CARTIS form application reveals an even distribution between masonry (MUR) and reinforced concrete (CAR) types, each comprising 40.0 % of the buildings. Reinforced concrete is the primary material for both horizontal (48.0 %) and roof structures (52.0 %), followed by steel.

2.2. The investigation of the historic centre urban sector (C02)

The study focuses on the historic centre of Meta (C02), where 452 buildings were identified, 378 of which are masonry structures. This urban sector shows considerable seismic vulnerability, as many buildings (84 %) are constructed with masonry, and most were built before 1950 (98 % of the buildings). Specifically, 89 % of the buildings were constructed before 1950, while only 11 % were built after 1950. This distribution reflects the historical development of Meta's urban fabric, with a strong presence of older structures that contribute to the area's cultural heritage but also present significant challenges in terms of seismic vulnerability. By consulting the building registry [13] and conducting supplementary on-site inspections using rapid analysis methods, an updated and comprehensive assessment of the building fabric in this sector is achieved.

A preliminary analysis indicates that masonry buildings make up most of the structures in the area, accounting for 84.1 % (see

Fig. 4. Curtains of buildings along (a) Via Olivari, (b)Via Santa Lucia and (c)Via A. Cosenza.

Fig. 4). Following this, a more thorough assessment of the masonry structures is conducted to categorize the specific types. Through on-site inspections, three distinct masonry typologies are identified (see Fig. 6) and labelled as MUR1, MUR2, and MUR3, as illustrated in Fig. 5.

The analysis continues with a focus on buildings that exclusively feature masonry structures, examining their characteristics and subsequently assessing their seismic vulnerability (see Fig. 6). The three observed masonry types reflect the region's historical building practices. The MUR1 type, which constitutes 76.8 % of the buildings, is characterized by regular masonry construction using uniform, square blocks of grey tuff, a material commonly found in the Campania region. The MUR2 type, comprising 4.2 % of the structures, consists of irregular masonry, where the grey tuff blocks exhibit an uneven shape. This suggests variations in material selection or construction techniques, possibly due to periods of material scarcity. The MUR3 type, making up 2.7 % of the buildings, features irregular masonry that incorporates a mix of grey tuff, limestone, and Massa stone, indicating a more complex and heterogeneous structure. This classification likely stems from specific architectural decisions or historical influences in the Campania region, offering valuable insights into the structural diversity of masonry buildings in Meta's historic center. It also aids in providing a more precise assessment of their seismic vulnerability.

Fig. 7 presents the GIS mapping and statistical analysis of the key structural characteristics of the surveyed buildings within the historic centre. The majority of the buildings date from the 18th (54 %) and 19th centuries (40 %). According to the 1998 census data [14], 71 % of the buildings feature vaulted horizontal structures. Many buildings also display a combination of different floor types, with vaults on the ground floors and steel, wood, or reinforced concrete used on the upper floors. Vaulted roofs remain the predominant roofing structure, accounting for 56.4 % of the buildings, highlighting the ongoing use of traditional vaulting alongside modern materials. When examining the number of floors, the data shows that 92 % of the structures have no more than three floors, reflecting the typical construction practices in historical urban areas.

2.3. Analysis of the identified typologies

In Sector 2 of Meta's historic centre, three different masonry types were identified, having specific material characteristics and distribution patterns as follows.

- MUR1 Typology: This typology includes 347 buildings, characterized by regular masonry constructed with square blocks of grey tuff. The majority of these buildings were built in the 1700s (53.6 %) and 1800s (39.5 %). They typically feature either two floors (48.4 %) or three floors (41.2 %), with cellars present in 27.4 % of cases. Vaulted floors are the predominant horizontal structure (70.6 %) and vaulted roofs are common (55.3 %). Most buildings are part of aggregated configurations (84.15 %). Renovations have occurred in 23.9 % of the buildings, 30.6 % are in good condition, and 40 % are in mediocre or poor condition. Wall connections are without tie rods in 74 % of cases, and structural irregularities are common, with 56.2 % showing irregularity in plan and 80.1 % in height.
- MUR2 Typology: This typology consists of 20 buildings constructed with irregular grey tuff masonry. Most of these buildings date back to the 1700s (68.4 %), with the remainder built in the 1800s (31.6 %). Vaults are prevalent in both the horizontal (68.4 %) and roof structures (63.2 %), often combined with iron elements. The majority of buildings are part of aggregated configurations (73.7 %). Renovations have occurred in 21 % of the buildings, 15.8 % are in good condition, while most (47.3 %) are in mediocre or poor condition, and 15.8 % are in very poor condition. Wall connections show variability, with tie rods present in 21 % of cases, absent in 68.4 %, and completely lacking in 10.6 %. Structural irregularities are widespread, with 73.7 % irregular in plan and 75 % irregular in height.

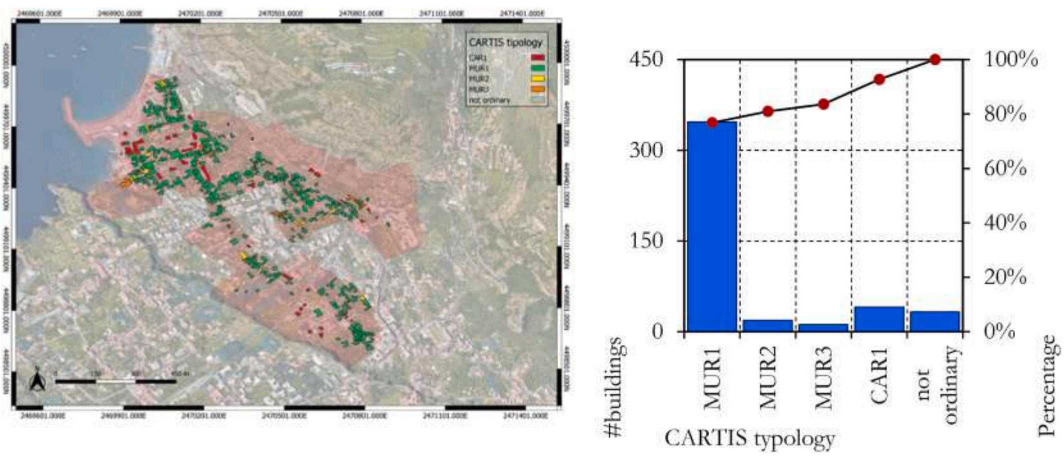

Fig. 5. GIS mapping and statistical elaboration of the CARTIS typologies within the inspected sector.

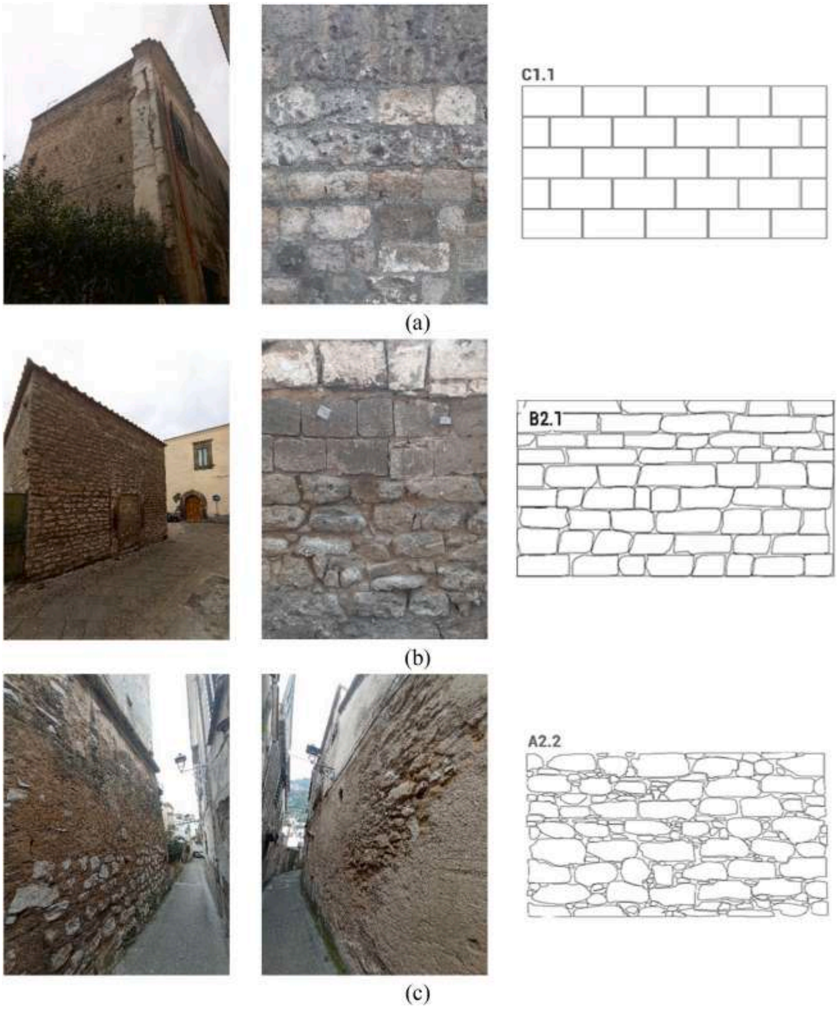

Fig. 6. Detailed photos of the masonry types (MUR1(a), MUR2 (b) and MUR3 (c)) identified by the AeDES Manual [18].

- MUR3 Typology: This typology includes only 12 buildings, characterized by irregular masonry consisting of grey tuff, limestone, and Massa stone. Most of these structures date back to the 1800s (66.7 %) and vary in height, with 50 % having two floors and some reaching four. Vaults are dominant in both horizontal and roof structures (75 %). Roofing typically combines multiple materials (91.7 %), and most buildings are part of aggregated configurations (75 %). The conservation state of these buildings is generally poor, with 66.7 % in mediocre or bad condition, and 33.3 % in very poor condition. Tie rods are present in 41.7 % of buildings, absent in 50 %, and 8.3 % lack any clamping. Structural irregularities are widespread, with 91.7 % exhibiting irregularity in plan and 83.3 % in height.

3. Large-scale vulnerability assessment

In this section, the vulnerability assessment is conducted using a structured methodological framework designed to characterize the likely seismic response of individual buildings within the historic urban sector of Meta. The previously collected data are analysed using the vulnerability index method initially developed by Benedetti and Petrini [23] and later refined by incorporating additional parameters proposed by Formisano et al. [10]. These additional parameters specifically address the interactions between adjacent buildings, enhancing the accuracy and precision of the assessment framework [20,22]. To facilitate this, a specialized form for aggregated buildings is employed (Table 1), enabling expert visual evaluations through weighted scores. A key aspect of this framework includes five supplementary parameters, extensively discussed in the literature [5,9], which further refine the evaluation by considering factors, such as the effects of building adjacency, structural irregularities, and local failure mechanisms. Recent research by Chieffo and Formisano [14], Mosoarca et al. [24], and Chieffo et al. [25] validated the significance of these parameters in strengthening the reliability of seismic vulnerability assessments. The parameters under investigation are outlined as follows.

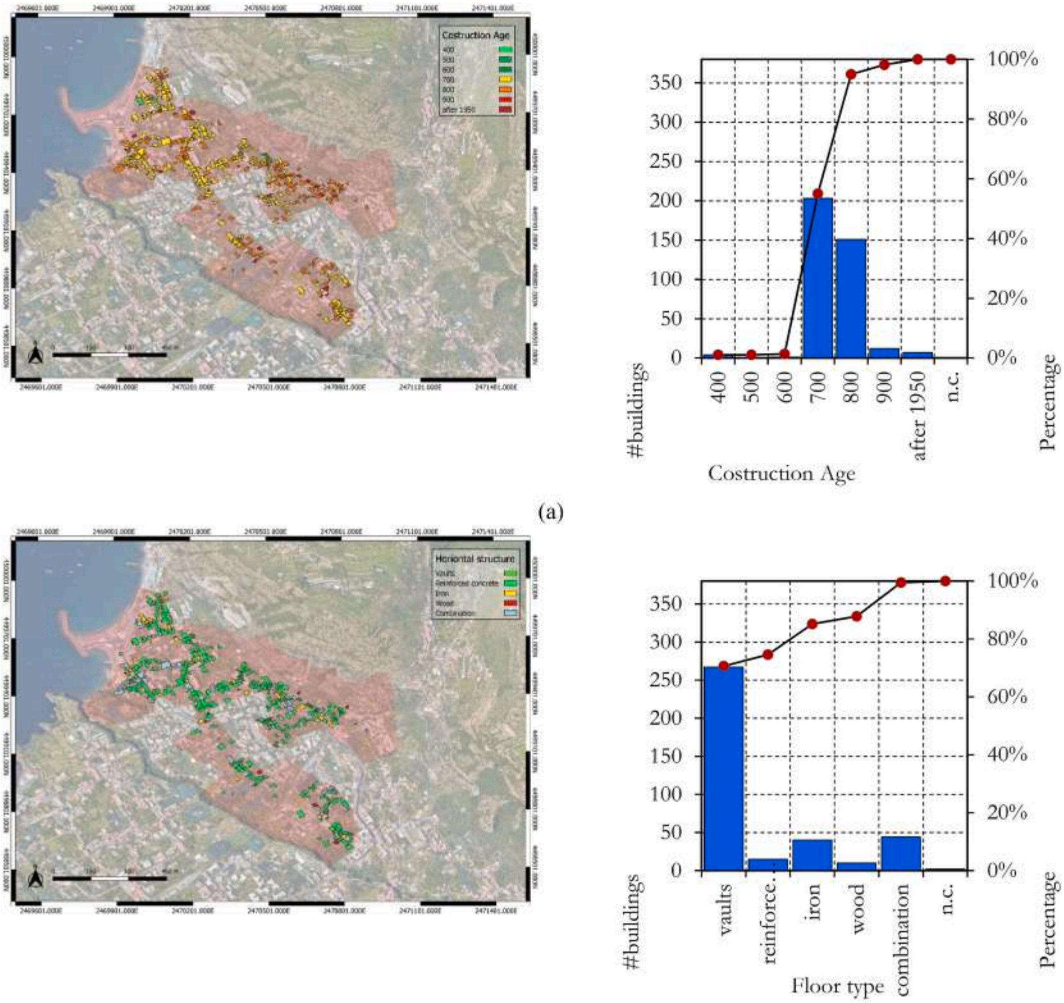

Fig. 7. GIS mapping and statistical elaboration of the main structural characteristics of masonry buildings within Sector 2: (a) construction age, (b) horizontal structure, (c) roofing structure, (d) number of floor, (e) basement floors

11. Height Difference with Adjacent Buildings: Variation in height between adjacent buildings negatively affects seismic response.
12. Position in Aggregate: This parameter considers plan interaction within the aggregate, classifying buildings as head, corner, or fully enclosed units.
13. Number of Staggered Floors: Staggered floors between adjacent buildings increase thrusts on shared elements, elevating stress levels.
14. Structural or Typological Heterogeneity: Homogeneous materials and techniques among adjacent buildings improve seismic behaviour, while heterogeneity heightens vulnerability.
15. Opening Area Differences: Significant differences in façade openings between adjacent buildings can alter seismic response.

These parameters, combined with the initial ten from Benedetti and Petrini's method [23], provide a comprehensive vulnerability index, calculated as follows:

$$I_V = \sum_{i=1}^{13} S_i \, . W_i \quad (1)$$

Subsequently, this index is normalized in the interval [0–1] as follows.

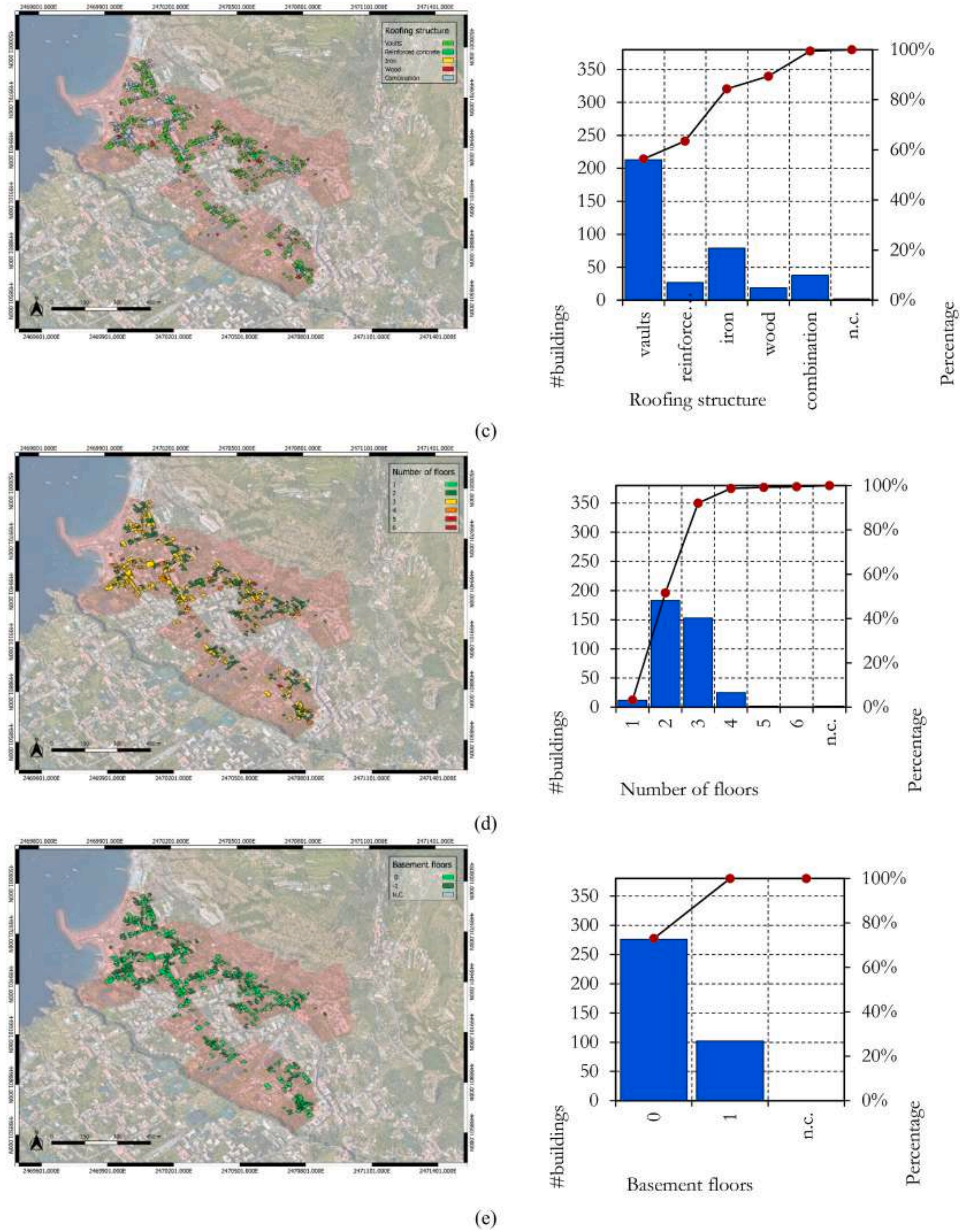

Fig. 7. (*continued*).

$$V_I = \left[\frac{I_V - \left(\sum_{i=1}^{15} S_{min}\ W_i\right)}{\left|\sum_{i=1}^{15} \left[(S_{max}\ W_i) - (S_{min}\ W_i)\right]\right|} \right] \tag{2}$$

This index provides a standardized measure of a building's susceptibility to damage. Thus, vulnerability values closer to 1 reflect the most vulnerable buildings, while values near 0 imply the presence of structures designed in conformity with recent seismic codes or subjected to retrofit interventions.

In Table 2, the significant data related to the normalized vulnerability index evaluated for buildings of the MUR1, MUR2 and MUR3 typologies, have been extrapolated.

Table 1
Vulnerability form for buildings in aggregate.

Parameters	Vulnerability classes				Weight
	A	B	C	D	
1. Organization of vertical structures	0	5	20	45	1
2. Nature of vertical structures	0	5	25	45	0,25
3. Location of the building and type of foundation	0	5	25	45	0,75
4. Distribution of plan resisting elements	0	5	25	45	1,5
5. In-plane regularity	0	5	25	45	0,5
6. Vertical regularity	0	5	25	45	0,8
7. Type of floor	0	5	25	45	0,8
8. Roofing	0	15	25	45	1
9. Details	0	0	25	45	0,25
10. Physical conditions	0	5	25	45	1
11. Presence of adjacent building with different height	−20	0	15	45	1
12. Position of the building in the aggregate	−45	−25	−15	0	1,5
13. Number of staggered floors	0	15	25	45	0,5
14. Structural or typological heterogeneity among adjacent SUs	−15	−10	0	45	1,2
15. Percentage difference of opening areas among adjacent facades	−20	0	25	45	1

In the above table VI_{mean} is the average vulnerability value, VI_{max} is the maximum vulnerability value, Vi_{min} is the smallest vulnerability value and VI* is the most frequent normalise vulnerability value within the analysed typology.

The vulnerability analysis reveals that the majority of buildings (300) exhibit medium vulnerability, accounting for 79.16 % of the total. The remaining buildings are classified as having medium-low vulnerability (15.57 %), medium-high vulnerability (4.75 %), and high vulnerability (0.53 %) (Fig. 8).

3.1. Typological vulnerability curves

For each identified building typology, typological vulnerability curves can be derived by using the mean value of the normalized vulnerability index and the standard deviation, both computed from the index values of the buildings. These curves predict the expected damage as a function of macroseismic intensity. The mathematical formulation of these curves is based on the equation developed by Lagomarsino and Giovinazzi [8]:

This formulation incorporates three principal factors:

$$\mu_D = 2.5\left[1 + \tanh\left(\frac{I + 6.25 \bullet V_I - 13.1}{Q}\right)\right] \tag{3}$$

- Normalized Vulnerability Index (VI): represents the intrinsic vulnerability of a building.
- Macroseismic Intensity (I): denotes the seismic intensity, as defined by the European Macroseismic Scale (EMS-98).
- Ductility Factor (Q): a variable coefficient ranging from 1 to 4, describing the energy dissipation capacity of different building classes. Higher values of Q correspond to increased ductility and reduced vulnerability. It is herein assumed as equal to 2.3 [8].

The equation allows for the derivation of average vulnerability curves for different building typologies, enabling the estimation of expected damage levels under varying earthquake intensities. These curves are instrumental in probabilistic seismic risk assessments and are frequently applied to evaluate the seismic vulnerability of masonry buildings. Numerous studies documented the successful implementation of this methodology, emphasizing its adaptability and robustness for large-scale applications [3,6,8,25]. In Figs. 9–11 the vulnerability curves derived for the three structural typologies are reported (y represents the standard deviation of the values). In Fig. 12 the comparison of the three mean curves is reported.

The MUR1 typology includes buildings built with square blocks of grey tuff, known for their stability and structural uniformity. Several studies, such as that of Ferretti et al. [20], indicate that the regularity and cohesion of the material offer a greater capacity to resist seismic stresses, as they reduce the variability of local responses under cyclic loads [6]. The vulnerability curve for MUR1 shows a less steep growth trajectory, indicating a potentially lower rate of vulnerability increase compared to MUR2 and MUR3. This means that MUR1 has a chance to only exceed damage levels D1 (light damage) and D2 (moderate damage) for higher intensities, demonstrating good overall resistance.

Table 2
Vulnerability index representative values.

Typology	VI_{mean}	VI_{max}	VI_{min}	VI*
MUR1	0,47	0,65	0,27	0,51
MUR2	0,52	0,82	0,40	0,49
MUR3	0,55	0,71	0,37	0,59

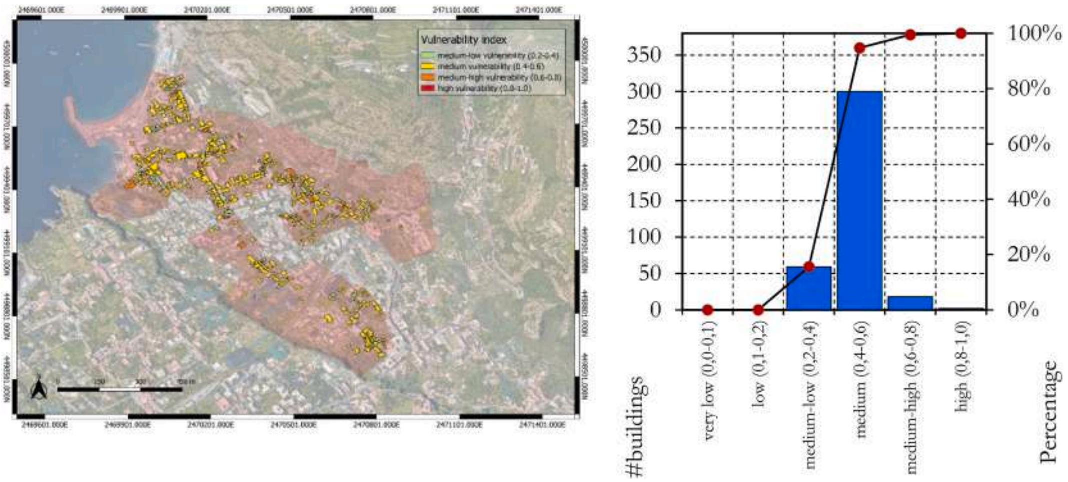

Fig. 8. Distribution of the Vulnerability Index in the examined area.

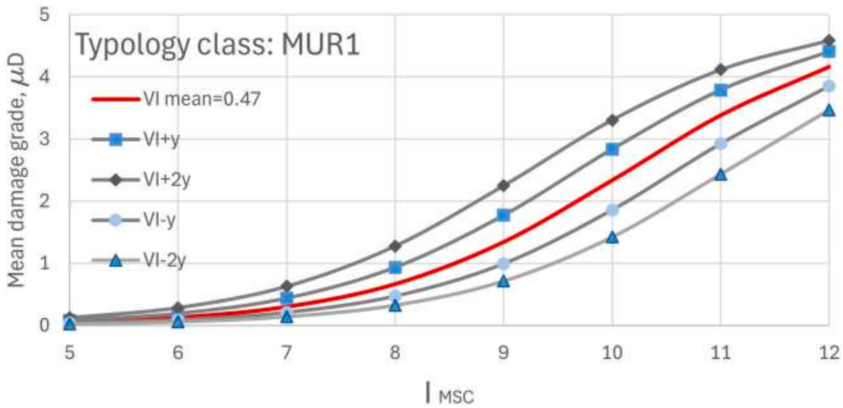

Fig. 9. Mean damage curves for the examined building typologies MUR1.

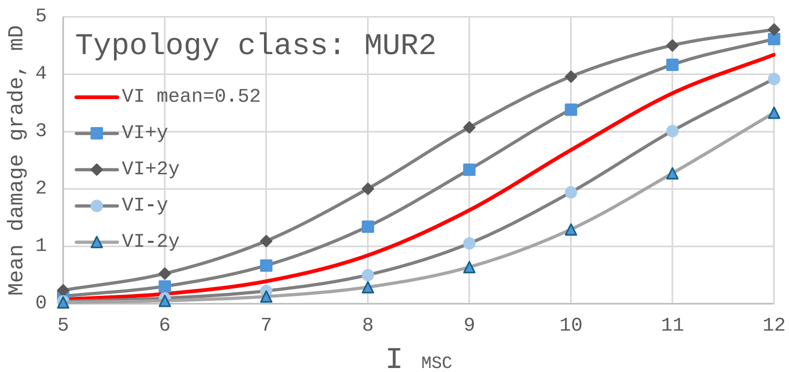

Fig. 10. Mean damage curves for the examined building typologies MUR2.

The spindle of the curves is narrow, suggesting that MUR1 buildings have a more predictable seismic response. Eslami et al. pointed out that homogeneous materials, such as square blocks of tuff, limit the variability of responses, reducing the uncertainty related to the properties of the material [22]. This makes MUR1 a type less susceptible at high damage under moderate seismic intensities.

Buildings belonging to the MUR2 type are composed of irregularly shaped tuff blocks, which introduce heterogeneity in the mechanical properties and in the distribution of forces. This type of construction presents a greater vulnerability to seismic loads due to the variability in the size and quality of mortar joints [14]. The vulnerability curve for MUR2 shows a probability of damage that starts

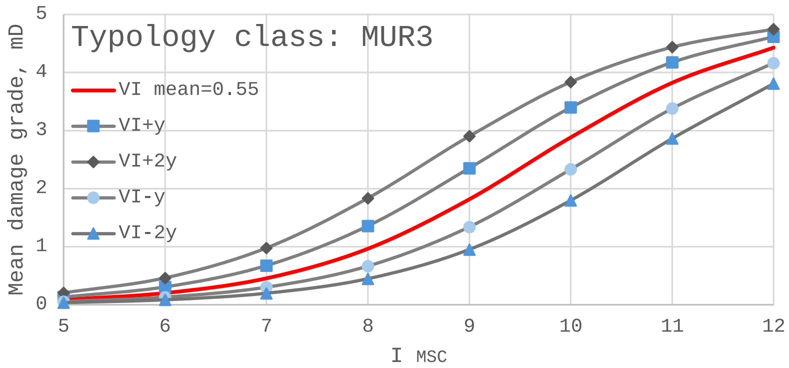

Fig. 11. Mean damage curves for the examined building typologies MUR3.

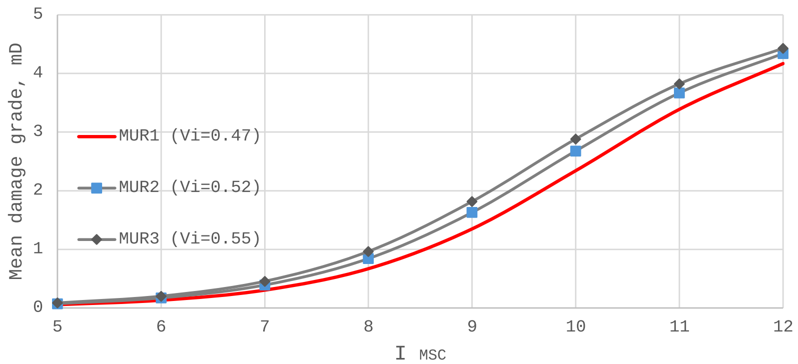

Fig. 12. Comparison of the average vulnerability curves for the three masonry types identified.

to increase at lower intensities than for MUR1. The presence of mortar joints of varying thickness and irregular stones impairs the ability to resist horizontal forces, increasing the likelihood of reaching damage levels D2 and D3 at moderate intensities. The variation in material quality creates weaknesses that can lead to localized damage during earthquakes [26]. The curves spindle of MUR2 is wider than that of MUR1, reflecting greater uncertainty. Benedetti and Petrini pointed out that irregularities in materials increase the variability in the response of masonry buildings during seismic events [23]. Therefore, MUR2 presents a less predictable response.

The MUR3 typology represents masonry buildings composed of a mixture of masonry materials, such as tuff, limestone and Massa stones. This combination creates a particularly heterogeneous and vulnerable structure. Research performed by Eslami et al. indicated that the mixture of materials with different strengths and properties led to an uneven and unpredictable distribution of forces [22].

Indeed, the vulnerability curve of MUR3 is the one with the greatest slope towards the highest damage levels already for moderate seismic intensities. This behaviour is consistent with the research of Lagomarsino and Giovinazzi [8]: structures composed of materials with different properties have a high risk of reaching D3 and D4 damage levels even for earthquakes of moderate intensity. The uneven properties make it difficult to evenly distribute stresses, increasing the risk of damage.

The spindle is very large for MUR3, reflecting a high variability in structural response. This variability is due to the inhomogeneity of the materials and the different interactions they have with seismic stresses. Formisano et al. pointed out that the combination of materials of varying density and strength increases the likelihood of uneven damage and partial collapse [10].

In Fig. 12 a comparison among the mean typological vulnerability curves derived for the three structural typologies is reported.

4. Damage scenarios

4.1. Damage model prediction

The seismic damage scenarios for the municipality of Meta are developed using data from the seismic hazard model MPS04-S1 [27], provided by the National Institute of Geophysics and Volcanology (INGV). This model offers probabilistic seismic hazard assessments, supplying key parameters to evaluate the potential impact of earthquakes on specific regions. The seismic hazard analysis focuses on the disaggregation of Peak Ground Acceleration (PGA) with a 10 % probability of exceedance over 50 years. The data, presented in Fig. 13, show the spatial and probabilistic distribution of PGA values for the area of interest. These values are crucial for estimating damage levels and for planning mitigation strategies to enhance structural and infrastructural resilience. Such analyses are fundamental for constructing accurate damage scenarios, as they directly inform vulnerability assessments and risk management strategies. When integrated with vulnerability curves, this data provides a more thorough understanding of the expected damage resulting from seismic events of varying intensities [28,29].

Passing to the application to the case study, to assess the damage scenario for Meta, it is essential to calculate the mean degree of damage (μ_D) for each building within the urban sector, based on the earthquake's magnitude and the epicentral distance. Thus, the initial step for applying (3) is to calculate the macroseismic intensity of the simulated event using the following formula [30]:

$$\mathrm{Log}(Y) = a + b \cdot Mw - c \cdot \log(D + c)\ F + S + y\ \log(Y) \tag{4}$$

where: Y,I: motion parameter (PGA - Y or Intensity - I); Mw: moment magnitude; D: epicentre distance (km); C: corrective attenuation factor; F: source parameter; S: site parameter; a,b,c: empirical coefficients; y: standard deviation of log(Y).

A simplified version for intensity calculation is derived as follows [29]:

$$I = a + b \cdot M_w - c \cdot \log(D + c) \tag{5}$$

This formula accounts for both the magnitude (M_W) and epicentral distance (D) of the simulated seismic event to model the seismic impact on building vulnerability. Each term in the formula has a specific role.

- Constant term a: represents a fixed offset, possibly reflecting baseline vulnerability influenced by intrinsic structural characteristics.
- Magnitude term b·Mw: increases the index with earthquake magnitude, suggesting that higher magnitudes have a greater effect on structures.
- Logarithmic term $-c \cdot \log(D + c)$: reduces the index value with increasing distance, helping model realistic attenuation of seismic effects. The parameter c prevents very low values of D from producing extreme or unstable results.

The simplified formula assumes the following values of a,b,c:

$$I = 6,39 + 1,756 \cdot M_w - 2,747 \cdot \log(D + 7) \tag{6}$$

Together, these terms allow for the modelling of the macroseismic intensity, *I*, as a function of earthquake magnitude and proximity, providing valuable insights into structural vulnerability under varying seismic conditions. The damage degree, μD, for each building is calculated using equation (3) [25], where IEMS−98 represents the intensity parameter derived from the previous calculation, VI is the normalized vulnerability index from the vulnerability assessment, and Q is a ductility factor, set at 2.3.

This calculation is applied to each building within the analysed sector. The actual damage level is then classified into specific intervals of damage degree (Table 3), which correspond to the type of structural damage based on the μD value obtained from the previous calculations.

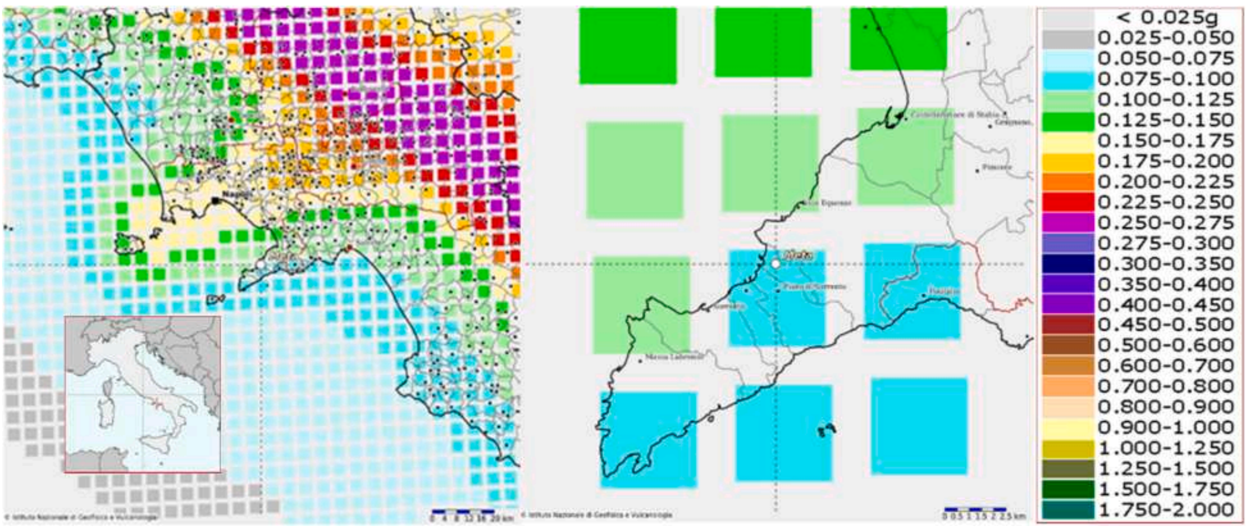

Fig. 13. Localization of the municipality of Meta in the INGV's MPS04-S model.

4.2. Results for analysed scenarios

In more detail, Fig. 14 presents six damage scenarios evaluated according to the disaggregation map. These scenarios consider seismic events with varying magnitudes and epicentral distances, as outlined below.

- **Scenario 1**: Magnitude M_w 4; Distance 20 km
- **Scenario 2**: Magnitude M_w 5; Distance 20 km
- **Scenario 3**: Magnitude M_w 6; Distance 20 km
- **Scenario 4**: Magnitude M_w 4; Distance 10 km
- **Scenario 5**: Magnitude M_w 5; Distance 10 km
- **Scenario 6**: Magnitude M_w 6; Distance 10 km

The related expected macroseismic intensities, calculated adopting the formulation proposed by Crespellani et al. (1998) [31], are reported in Table 4.

These damage scenarios provide a comprehensive view of how varying seismic intensities and epicentral distances impact building damage distribution across Meta's historic centre.

In addition, Damage Probability Matrices (DPM) are derived and evaluated based on the weighted average of damage, μ_D, according to the following equation:

$$\begin{cases} P_k = \dfrac{5!}{k!(5-k)!}\left(\dfrac{\mu_D}{5}\right)^k\left(1-\dfrac{\mu_D}{5}\right)^{5-k} \\ \mu_D = \displaystyle\sum_{k=1}^{5} P_k\, k \end{cases} \tag{7}$$

where k, representing the numerical-functional parameter associated with different levels of damage, ranges from 0 to 5 and indicates the potential severity of damage as defined in a classification system [32], while pk is the probability or statistical frequency of experiencing a damage level k.

By calculating μ_D for each building, it becomes possible to estimate the overall vulnerability and damage distribution within Meta's historic centre under various seismic scenarios (Fig. 14). This methodology provides actionable data for urban resilience planning, allowing for targeted retrofitting strategies [30].

5. Fragility assessment

The seismic vulnerability assessment conducted for the examined area integrates fragility curves to quantitatively evaluate the susceptibility of buildings to varying seismic intensities. These curves establish a relationship between ground motion indicators, such as macroseismic intensity or Peak Ground Acceleration (PGA), and the probability of reaching or exceeding specific structural damage levels. The EMS-98 scale is effective for assessing vulnerability across different building types by correlating macroseismic intensity with observed damage levels. However, it has limitations in scenario analyses and seismic risk evaluations, where PGA is often the preferred input parameter [33].

To address this limitation, Lagomarsino and Cattari [36] proposed a correlation between macroseismic intensity and PGA. While variability exists among different correlations due to variations in urban environments and seismic event characteristics, this method offers a practical approach [34]. Empirical fragility curves, such as those developed by Del Gaudio et al. [26] and Zucconi et al. [35], use post-earthquake data (e.g., from the 2009 L'Aquila earthquake) to model the vulnerabilities of unreinforced masonry (URM) buildings specifically.

For this study, fragility curves are generated using an intensity-to-PGA correlation expressed as:

$$\log(\mathrm{PGA}) = a \cdot I + b \tag{8}$$

that could be converted in:

$$\log(\mathrm{PGA}) = c_1 \cdot I - c_2 \ (\text{PGA expressed in g}) \tag{9}$$

Table 3
Damage levels adopted.

Damage range, μD	Damage state (EMS-98)	Damage level
0–0.5	D0	No damage
0.5–1.0	D1	Negligible
1.0–2.0	D2	Moderate
2.0–3.0	D3	Substantial
3.0–4.0	D4	Partial collapse
4.0–5.0	D5	Collapse

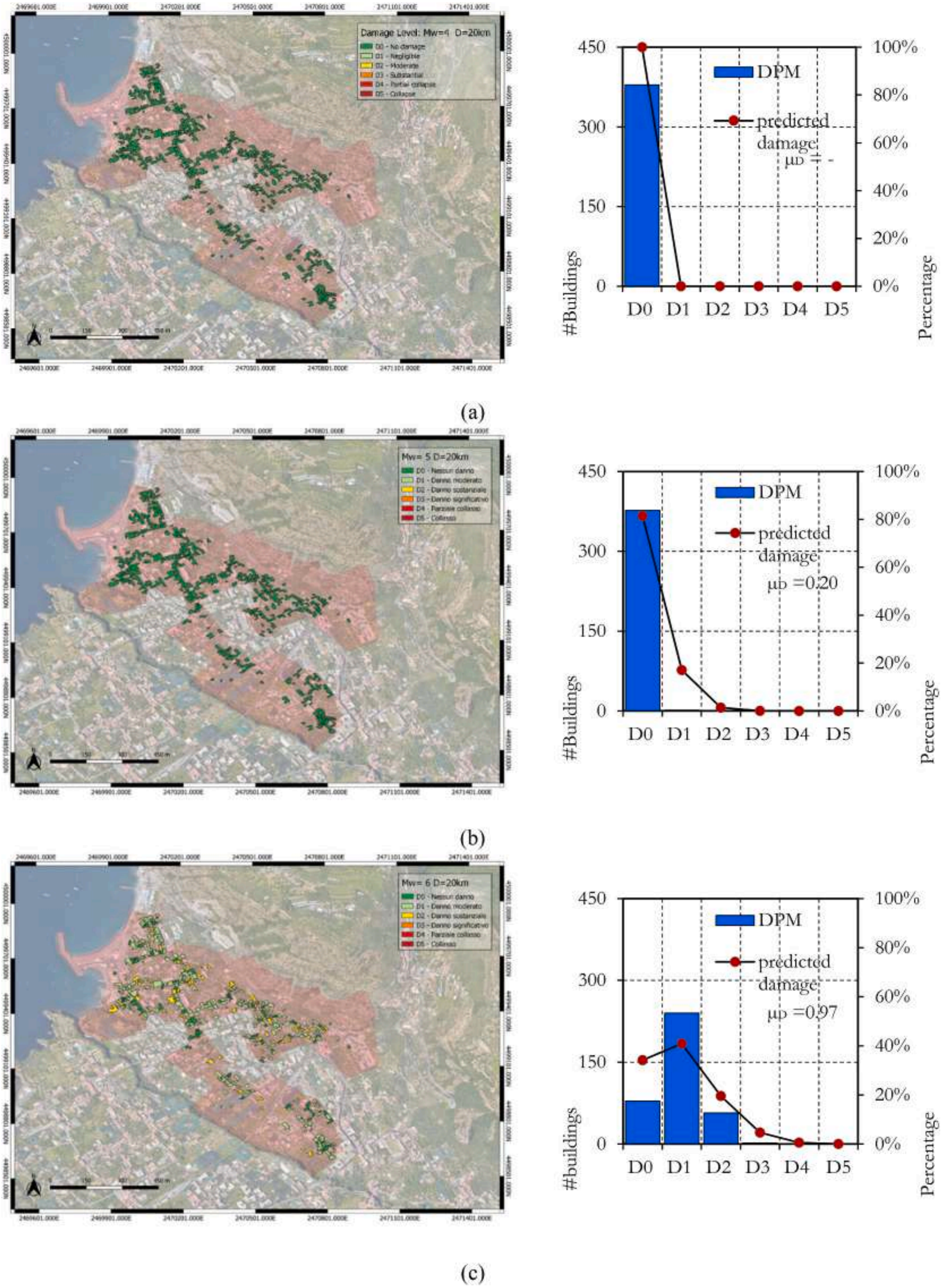

Fig. 14. Damage scenarios: a) M_w:4; D:20 km, b) M_w:5; D:20 km, c) M_w:6; D:20 km, d) M_w:4; D:10 km, e) M_w:5; D:10 km, f) M_w:6; D:10 km

where $c_1 = 0.602$ and $c_2 = 7.073$ are empirical coefficients calibrated from past Italian earthquake data. Here, I represents the macroseismic intensity, while PGA is expressed in g [36].

Adopting a macroseismic approach, the fragility curves for the analysed building typologies are derived using a binomial distribution function. This function calculates the probability of exceeding a given damage level Dk (k = 0,1, …,5) based on the average

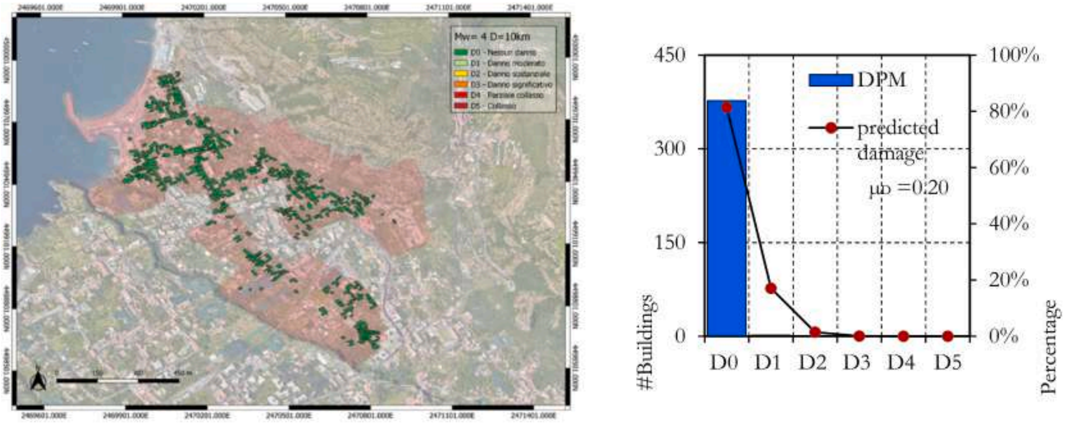

(d)

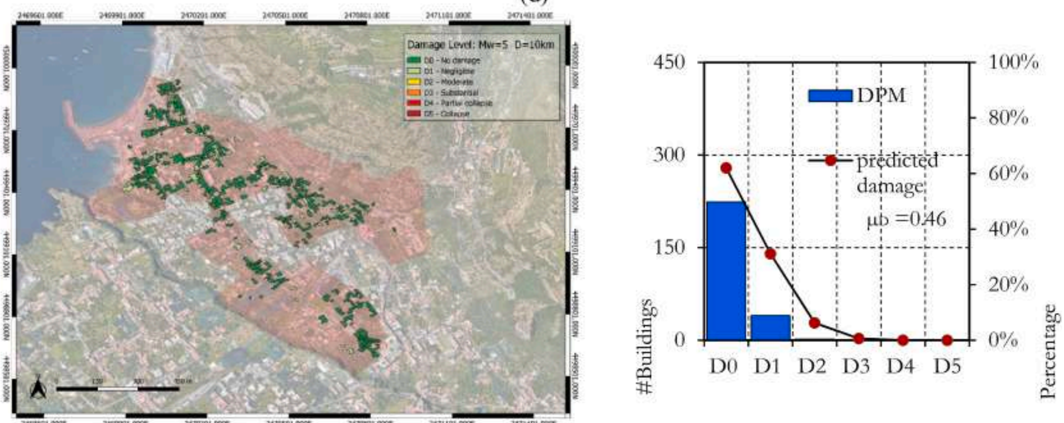

(e)

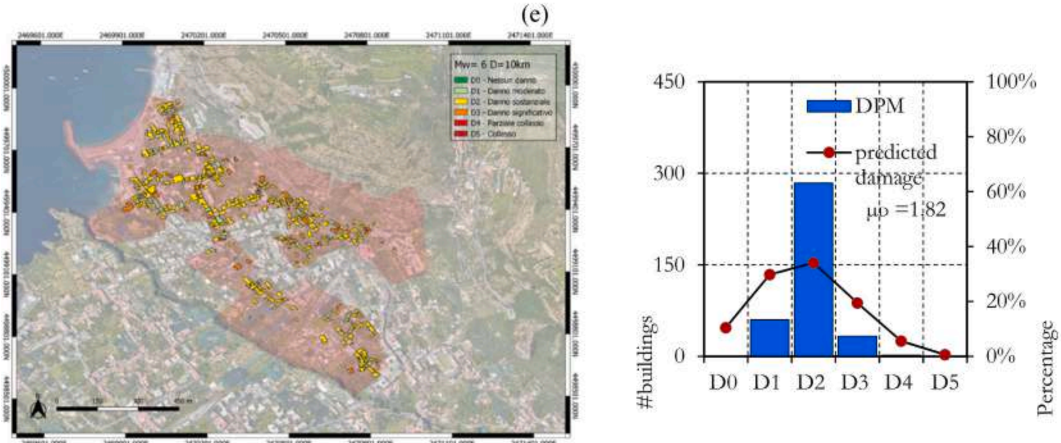

(f)

Fig. 14. (*continued*).

Table 4
Expected macroseismic intensities adopting the formulation proposed by Crespellani et al. [31].

Magnitude, M_w	Macroseismic Intensity, I	
	R = 10 km	R = 20 km
4.0	VI	–
5.0	VII	VI
6.0	IX	VIII

damage μ_D, constrained by $0 \leq \mu_D \leq 5$ [22]. For each macroseismic intensity level, the cumulative probability mass function is calculated to derive the fragility functions, as follows:

$$P(Di \geqslant Dk|I) = \sum_{k=1}^{5} pk \quad (10)$$

These fragility functions, plotted in Fig. 15, provide a probabilistic framework to assess the likelihood of damage levels for the examined typologies, supporting scenario-based analyses and risk management strategies in seismically active regions.

The fragility curve for MUR1, which represents buildings constructed with regular masonry using square blocks of tuff, exhibits a gradual slope. This indicates a low probability of exceeding higher damage levels (D3 and D4) until high seismic intensities are reached. The regularity and cohesion of the materials contribute to a uniform structural behaviour, ensuring an even distribution of seismic stresses [19,23]. The curve reflects low variability in response, suggesting predictable structural behaviour. However, MUR1 buildings are not immune to severe damage under high seismic intensities, implying that minimal consolidation measures could improve resilience in high-risk areas.

The fragility curve for MUR2 demonstrates a steeper increase in damage probability, even at moderate seismic intensities, indicating greater vulnerability compared to MUR1. These buildings, constructed with irregularly shaped tuff blocks, lack uniform cohesion, introducing structural weaknesses. As a result, the probability of exceeding damage levels D2 and D3 becomes significant during medium-intensity earthquakes. This behaviour is consistent with findings by Mosoarca et al., who highlight the detrimental effects of irregular materials and variable mortar joints on lateral resistance capacity [14,24]. The broader spindle of the MUR2 fragility curve reflects greater variability in seismic response, mirroring the heterogeneity of materials and uneven force distribution. To address this increased vulnerability, reinforcement interventions are crucial to improve seismic stability.

The fragility curve for MUR3 shows the steepest slope, indicating a high probability of exceeding significant damage levels (D3 and D4) even at low to moderate seismic intensities. This typology, characterized by a mix of materials including tuff, limestone, and Massa stone, exhibits substantial heterogeneity in mechanical properties. This variability leads to stress concentrations at weaker points, increasing the likelihood of severe damage or collapse. The wide spindle of the curve reflects significant uncertainty in seismic response due to uneven force distribution. Studies by Lagomarsino and Giovinazzi [8] and Eslami et al. [22] support these findings, highlighting the high vulnerability of mixed-material masonry structures. Buildings of the MUR3 type require substantial structural consolidation to mitigate potential damage.

The comparison among the different masonry typologies in terms of fragility curves is depicted in Fig. 16.

The analysis of the fragility curves reveals distinct patterns of vulnerability across the three building typologies. MUR1, known for its structural regularity and cohesive construction with square tuff blocks, shows the lowest probability of severe damage (e.g., D3 and D4) under moderate seismic intensities. In contrast, MUR2 and MUR3 exhibit significantly higher risks of exceeding severe damage thresholds, even at lower seismic intensities. The irregular construction of MUR2, with its inconsistent tuff blocks and weak mortar joints, leads to a higher likelihood of moderate to severe damage. MUR3, with its mixed-material composition, proves to be the most vulnerable, displaying steep fragility curves and significant uncertainty in seismic response due to its heterogeneous mechanical properties. These findings highlight the critical role of structural and material uniformity in determining seismic resilience.

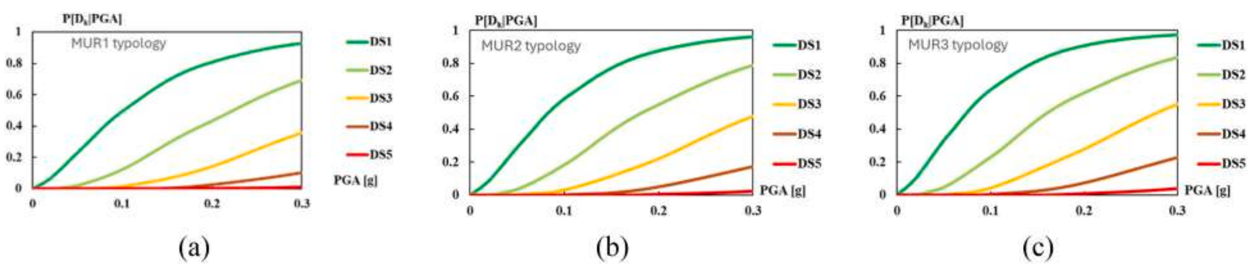

Fig. 15. Fragility curves for a) MUR1, b) MUR2 and c) MUR3 typologies.

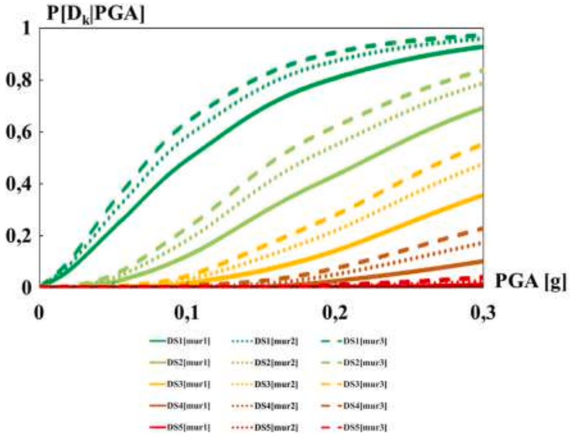

Fig. 16. Comparison among the various masonry types identified in terms of fragility curves.

6. Conclusions

This study provided an in-depth analysis of the seismic vulnerability of masonry structures in the historic centre of Meta, highlighting how different masonry typologies may respond to seismic events. The results indicated that buildings with regular masonry (MUR1) exhibit greatest resilience, especially in moderate earthquake scenarios, whereas the MUR2 and MUR3 typologies, marked by structural irregularities and material variability, demonstrate higher vulnerability levels. The use of fragility curves and vulnerability indices enabled a quantitative assessment of risk and provided reliable damage estimates, supporting decision-making for risk mitigation.

The analysis confirmed the need for targeted retrofitting to reduce seismic risks in historic centres, for example in buildings with structural characteristics similar to those examined in Meta. The findings emphasized the critical relationship between structural features of buildings, earthquake magnitude and epicentral distance in determining the severity of structural damage. Traditional masonry buildings in Meta, such as those with vaulted floors and irregular masonry, are especially vulnerable to seismic forces. The analysis also confirmed the decisive role of seismic intensity and epicentral proximity in influencing damage severity. For example, in scenarios involving a magnitude 6 earthquake within a 10 km radius, the damage observed was significantly greater than in lower-magnitude or more distant events. This disproportionate increase aligned with nonlinear seismic response models, such as those proposed by Lagomarsino and Giovinazzi [8], and illustrates how small variations in seismic intensity can result in substantial increases in structural damage.

Architectural characteristics, such as aggregated building configurations and composite masonry, further exacerbated vulnerability. These features, common in historic centres like Meta, led to irregular load distributions under seismic stress, amplifying structural deficiencies. Similar vulnerabilities were documented in studies carried out by Cima et al. [37] and Zucconi et al. [38], highlighting the challenges posed by historical construction techniques in seismically active regions. These studies emphasized that even moderate increases in seismic intensity can lead to significant damage augments in unreinforced masonry buildings, underscoring the necessity for ongoing assessments and targeted interventions [35]. In Meta's historic centre, the dense clustering of vulnerable buildings added an additional layer of complexity to seismic risk assessment. Close proximity among structures amplified interaction effects, increasing the likelihood of cascading failures during significant seismic events. This phenomenon, as noted by Mosoarca et al. [24], underscored the importance of detailed seismic vulnerability assessments to inform urban planning and disaster preparedness strategies.

The fragility curves and damage probability matrices developed in this study provided critical tools for understanding and forecasting the seismic impacts on Meta's historic buildings. Further research could expand on this study, for example, by incorporating numerical models or continuous monitoring methods to achieve more precise seismic behaviour predictions. Monte Carlo simulations could also be developed as further advancement of this study to account for uncertainty in input parameters during vulnerability analysis. Additionally, expected losses and retrofitting strategies can be incorporated, along with the validation of damage scenarios using recorded data. Protecting and restoring these historic structures is essential to safeguarding architectural and cultural heritage and should be a priority in urban planning for seismically active regions.

CRediT authorship contribution statement

Luigi Amitrano: Writing – original draft, Investigation, Formal analysis, Data curation. **Roberta Di Chicco:** Writing – original draft, Investigation, Formal analysis. **Antonio Formisano:** Writing – review & editing, Validation, Supervision, Project administration, Methodology, Conceptualization.

Declaration of competing interest

The authors declare that they have no known competing financial interests or personal relationships that could have appeared to influence the work reported in this paper.

Acknowledgments

The Authors would like to acknowledge the DPC-ReLUIS 2024–2026 research project (WP4 research line) for the financial support to the current research activity.

Data availability

Data will be made available on request.

References

[1] L. Sorrentino, S. Cattari, F. da Porto, G. Magenes, A. Penna, Seismic behaviour of ordinary masonry buildings during the 2016 central Italy earthquakes, Bull. Earthq. Eng. 17 (10) (2019) 5583–5607.
[2] D.F. D'Ayala, S. Paganoni, Assessment and analysis of damage in L'Aquila historic city centre after 6th April 2009, Bull. Earthq. Eng. 9 (1) (2011) 81–104.
[3] M. Dolce, A. Kappos, G. Magenes, Seismic vulnerability of masonry structures and urban systems, J. Earthq. Eng. 20 (2016) S1–S11.
[4] INGV (National Institute of Geophysics and Volcanology) https://rischi.protezionecivile.gov.it/it/sismico/attivita/classificazione-sismica/.
[5] R. Di Chicco, N. Chieffo, A. Formisano, Exposure and seismic vulnerability of masonry buildings grouped in aggregate of a typical historical centre in the Basilicata region of Italy, J. Build. Eng. 94 (2024) 109859.
[6] G. Milani, M. Valente, Failure analysis of historical masonry structures under seismic actions: a review, Eng. Fail. Anal. 47 (2015) 154–169, https://doi.org/10.1016/j.engfailanal.2014.10.013.
[7] ReLUIS, Development of a systematic methodology for exposure assessment at a territorial scale based on typological/structural characteristics of buildings, Research project report (2014–2016).
[8] S. Lagomarsino, S. Giovinazzi, Macroseismic and mechanical models for the vulnerability and damage assessment of current buildings, Bull. Earthq. Eng. 4 (4) (2006) 415–443, https://doi.org/10.1007/s10518-006-9024-z.
[9] S. Lagomarsino, S. Cattari, D. Ottonelli, The heuristic vulnerability model: fragility curves for masonry buildings, Bull. Earthq. Eng. 19 (2021) 3129–3163.
[10] A. Formisano, G. Florio, R. Landolfo, F.M. Mazzolani, Numerical calibration of an easy method for seismic behaviour assessment on large scale of masonry building aggregates, Adv. Eng. Software 80 (2015) 116–138, https://doi.org/10.1016/j.advengsoft.2014.09.013.
[11] Z.V. Milutinovic, G.S. Trendafiloski, Risk-UE an Advanced Approach to Earthquake Risk Scenarios with Applications to Different European Towns, Contract: EVK4-CT-2000-00014, WP4, Vulnerability of Current Buildings, 2003.
[12] QGIS Development Team, QGIS Geographic Information System, Open Source Geospatial Foundation Project, 2014. http://qgis.osgeo.org.Qgisorg. http://www.qgis.org/.
[13] Municipality of Meta, Building Registry and General Plan (PRG). Municipality Records, 1998.
[14] N. Chieffo, A. Formisano, Geo-hazard-based approach for the estimation of seismic vulnerability and damage scenarios of the old city of Senerchia (Avellino, Italy), Geosciences 9 (2) (2019) 59, https://doi.org/10.3390/geosciences9020059.
[15] ISTAT, Population data, Web link: http://dati.istat.it/Index.aspx?QueryId=18563, 2021.
[16] CARTIS Form, Typological and Structural Building Characterization Methodology. Project Methodology Document, 2023.
[17] Department of Civil Protection (DPC), National seismic and volcanic risk assessment office, PLINIVS/LUPT Study Centre (2021).
[18] C. Baggio, A. Bernardini, R. Colozza, L. Corazza, Manuale per la compilazione della scheda di 1 livello di rilevamento danno, pronto intervento e agibilità per edifici ordinari nell'emergenza post-sismica, Editrice Italiani Nel Mondo Srl-Roma (2009).
[19] F. Puncello, S. Caprili, Seismic assessment of masonry vaults and lateral resistance under seismic loading, J. Struct. Eng. 56 (4) (2023) 234–245.
[20] F. Ferretti, G. Rossi, S. Bellucci, Fragility and resistance of masonry buildings under seismic loads: a comparative study of construction types, Earthq. Eng. Struct. Dynam. 49 (2) (2024) 312–329.
[21] M. Mercuri, M. Pathirage, A. Gregori, G. Cusatis, Masonry vaulted structures under spreading supports: analyses of fracturing behavior and size effect, J. Build. Eng. 45 (2022) 103396.
[22] A. Eslami, M. Della Mora, G. Milani, Seismic behavior of masonry structures with reinforced concrete floors: case studies and experimental approaches, Constr. Build. Mater. 23 (3) (2009) 784–792.
[23] D. Benedetti, V. Petrini, Sulla vulnerabilità sismica di edifici in muratura: Un metodo di valutazione, L'Industria delle Costruzioni 149 (1984) 66–74.
[24] M. Mosoarca, D. Bostenaru, D. Dumitrescu, Seismic vulnerability assessment of heritage buildings in Europe, J. Cult. Herit. 38 (2019) 126–136.
[25] M. Zucconi, R. Ferlito, L. Sorrentino, Simplified survey form of unreinforced masonry buildings calibrated on data from the 2009 L'Aquila earthquake, Bull. Earthq. Eng. 16 (7) (2018) 2877–2911, https://doi.org/10.1007/s10518-017-0283-7.
[26] C. Del Gaudio, G. De Martino, P. Ricci, G.M. Verderame, Empirical fragility curves for Italian URM buildings, Bull. Earthq. Eng. 15 (4) (2017) 1425–1450.
[27] INGV (National Institute of Geophysics and Volcanology) Seismic hazard model. Web link: https://esse1-gis.mi.ingv.it/.
[28] H. Crowley, R. Pinho, Simplified equations for estimating the seismic vulnerability of existing buildings, J. Earthq. Eng. 14 (1) (2010) 1–18.
[29] Working Group MPS, Drafting of the Seismic Hazard Map provided for by Ordinance PCM 3274 and its Subsequent Amendments, INGV, Rome, Italy, 2004 (in Italian).
[30] D. Albarello, V. D'Amico, M. Mucciarelli, Probabilistic seismic hazard assessment in Italy, J. Seismol. 12 (1) (2008) 23–41.
[31] S. Crespellani, R. Catenacci, L. Luzi, Macroseismic intensity and damage, J. Seismol. 2 (1) (1998) 41–55.
[32] S. Giovinazzi, S. Lagomarsino, A macroseismic method for the vulnerability assessment of buildings. 13th World Conference on Earthquake Engineering, 2004. Paper No. 896.
[33] N. Chieffo, A. Formisano, T.M. Ferreira, Damage scenario-based approach and retrofitting strategies for seismic risk mitigation: an application to the historical Centre of Sant'Antimo (Italy), European Journal of Environmental and Civil Engineering 25 (11) (2021) 1929–1948, https://doi.org/10.1080/19648189.2019.1596164.
[34] S. Lagomarsino, S. Cattari, D. Ottonelli, The heuristic vulnerability model: fragility curves for masonry buildings, Bullettin of Earthquake Engineering 19 (2021) 3129–3163.

[35] M. Zucconi, M. Di Ludovico, L. Sorrentino, Census-based typological usability fragility curves for Italian unreinforced masonry buildings, Bull. Earthq. Eng. 20 (8) (2022) 4097–4116, https://doi.org/10.1007/s10518-022-01361-8.
[36] S. Lagomarsino, S. Cattari, Fragility functions of masonry buildings (Chapter 5), in: K. Pitilakis, H. Crowley, A.M. Kaynia (Eds.), SYNER-G: Typology Definition and Fragility Functions for Physical Elements at Seismic Risk: Elements at Seismic Risk, Geotechnical, Geological and Earthquake Engineering 27 (2014) 111–156, https://doi.org/10.1007/978-94-007-7872-6_5.
[37] S. Szabó, M.F. Funari, P.B. Lourenço, Masonry patterns' influence on the damage assessment of URM walls: current and future trends, Developments in the Built Environment 13 (2023) 100119, https://doi.org/10.1016/j.dibe.2023.100119.